

**NASA TECHNICAL
MEMORANDUM**

NASA TM X-52800

N70-27960

NASA TM X-52800

**CASE FILE
COPY**

**ANOMALOUS BEHAVIOR OF LIQUID
NITROGEN DROPS IN FILM BOILING**

by Kenneth J. Baumeister, Edward G. Keshock,
and Donald A. Pucci
Lewis Research Center
Cleveland, Ohio

TECHNICAL PAPER GS for presentation at
Cryogenic Engineering Conference sponsored by the
National Academy of Science/National Research Council
Boulder, Colorado, June 17-19, 1970

ANOMALOUS BEHAVIOR OF LIQUID NITROGEN DROPS IN FILM BOILING

by Kenneth J. Baumeister, Edward G. Keshock, and Donald A. Pucci

**Lewis Research Center
Cleveland, Ohio**

TECHNICAL PAPER G3 for presentation at

**Cryogenic Engineering Conference
sponsored by the National Academy of Science/National Research Council
Boulder, Colorado, June 17-19, 1970**

NATIONAL AERONAUTICS AND SPACE ADMINISTRATION

ANOMALOUS BEHAVIOR OF LIQUID NITROGEN DROPS IN FILM BOILING

by Kenneth J. Baumeister,^{*} Edward G. Keshock,[†] and Donald A. Pucci[‡]

Lewis Research Center
National Aeronautics and Space Administration
Cleveland, Ohio

ABSTRACT

The vaporization time of large drops of ordinary fluids such as water, ethanol, or benzene have been correlated by conventional laminar film boiling theory. However, liquid nitrogen data has been found to have a 30 percent shorter vaporization time than predicted by theory. Experimental and theoretical attempts are made herein to resolve this discrepancy.

An asymptotic expression for the vaporization time of large drops in film boiling has been derived. This expression seems to correlate the nitrogen data. Also, a new expression for the modified latent heat of vaporization is derived. This expression is useful for large temperature gradients occurring within the vapor film supporting the drop or for fluids having small latent heats such as would occur for cryogenics or ordinary fluids near the thermodynamic critical point.

NOMENCLATURE

A	area
A*	dimensionless area, see table I, A/L^2
C _p	specific heat at constant pressure
f	radiation correction factor (given in ref. 5)
g	acceleration of gravity

^{*}NASA Lewis.

[†]Old Dominion University.

[‡]Cleveland State University.

g_c	gravitational constant
h	heat transfer coefficient
h^*	dimensionless heat transfer coefficient (see table I)
h_{fp}	heat transfer coefficient from flat plate
h_{fp}^*	dimensionless h_{fp}
k	thermal conductivity
L	$[\sigma g_c / (\rho_L - \rho_v) g]^{1/2}$
l	drop thickness (see table I)
l^*	dimensionless drop thickness (see table I), l/L
r	radial coordinate
T	temperature
ΔT	$T_p - T_{sat}$
T_p	plate temperature
T_{sat}	saturation temperature
t	total vaporization time
t^*	dimensionless vaporization time, see table I
V	drop volume
V^*	dimensionless drop volume, see table I, V/L^3
z	axial coordinate
α	thermal diffusivity
β	dimensionless gap thickness, eq. (15)
δ	gap thickness
δ^*	dimensionless gap thickness, see table I
η	dummy variable
λ	latent heat of vaporization
λ^*	modified latent heat of vaporization

λ^+ modified latent heat of vaporization for calculation of vapor gap thickness

$$(1) \lambda^+ = \lambda \left(1 + \frac{7}{20} \frac{C_p \Delta T}{\lambda} \right) \quad \text{from reference 9 for small values}$$

$$(2) \lambda^+ = \frac{C_p \Delta T}{\beta} = \lambda \left(\frac{\lambda^*}{\lambda} \right)^{-1/3} \quad \text{for large } C_p \Delta T / \lambda \quad \text{from}$$

present paper

λ_{cr}^* approximate expression for λ^* for $(C_p \Delta T / \lambda) > 2$

λ_{max}^* least upper bound of λ^*

λ_{small}^* approximation to λ^* for small $C_p \Delta T / \lambda$

μ viscosity

ρ_L liquid density

ρ_v vapor density

σ surface tension

ω axial velocity

INTRODUCTION

Film boiling of liquid drops, called Leidenfrost boiling, plays an important role in energy transfer in cryogenic systems. Leidenfrost boiling occurs when a liquid drop rests on a cushion of its own vapor resulting from heat transfer from a hot supporting surface. For a listing of recent publication and more details on the physics of Leidenfrost boiling, the reader may refer to references 1, 2, or 3 which contain a comprehensive literature summary of Leidenfrost boiling.

A recent paper by Forslund and Rohsenow (ref. 4) recognized the importance of Leidenfrost boiling in either nuclear or conventionally fired boiler tubes. They used the correlations developed by Baumeister, Hamill, and Schoessow (ref. 5) for predicting the heat transfer coefficients in the Leidenfrost boiling portion of the boiler tube. The correlations of reference 5 for the dimensionless average drop thickness l^* , area A^* , heat

transfer coefficient to the drop h^* , and total vaporization t^* are shown in table I of this report and will be referred to periodically. All these parameters are a function of the initial dimensionless volume of liquid V^* placed on the hot surface.

The dimensionless vaporization time t^* in table I represents the dimensionless time for a drop of dimensionless volume V^* to completely vaporize. The equations in table I have been found to correlate conventional fluids such as water, ethanol, benzene, or carbon tetrachloride. However, Keshock and Bell (ref. 1) showed that liquid nitrogen Leidenfrost data fell 30 percent below the theoretical curve, although the data did follow the general trend predicted by the theory.

Keshock and Bell (ref. 1) showed that the actual heat transfer coefficient was about 30 percent higher than that predicted by the equations in table I. This accounts for the shorter vaporization times. They attributed this increase in heat transfer rate to vapor instabilities. At large dimensionless liquid volumes ($V^* > 155$), the vapor beneath the liquid drop breaks through the surface of the liquid. This effect is not considered in the theory and could account for the shift downward of the data.

Baumeister (ref. 6) suggested a second possible explanation for nitrogen data falling below the theoretical curve. In the theory used to develop the equations in table I, an asymptotic expansion is introduced to account for the convection terms in the energy equation. This expansion is good only under the condition that

$$\frac{C_p(T_p - T_{\text{sat}})}{\lambda} \ll 1 \quad (1)$$

The parameter λ is the latent heat of vaporization and $(T_p - T_{\text{sat}})$ is the plate temperature minus the saturation temperature, while C_p is the specific heat at constant pressure. The expansion leads to a formula for a modified latent heat of vaporization of the form

$$\lambda_{\text{small}}^* = \lambda \left[1 + \frac{7}{20} \frac{C_p(T_p - T_{\text{sat}})}{\lambda} \right]^{-3} \quad (2)$$

The asymptotic expansion used to develop equation (2) is applicable to

ordinary fluids since λ is generally greater than the product of $C_p(T_p - T_{sat})$. However, nitrogen has a much smaller value of the latent heat than other fluids. Consequently, the expression for the modified latent heat of vaporization could be in error since equation (1) is no longer satisfied, and a corrected value might improve the agreement between experiment and theory.

Furthermore, at pressures approaching the critical pressure, equation (2) may lead to large errors since the ratio of $C_p(T_p - T_{sat})/\lambda$ approaches infinity. The energy equation should be investigated to see what effect large values of $C_p(T_p - T_{sat})/\lambda$ have on the expression for λ^* .

The purpose of this paper is as follows:

(1) First, to experimentally investigate the hypothesis put forward by Keshock and Bell concerning the effect of vapor instabilities on the total vaporization time of large sheets of liquid undergoing film boiling. Vaporization time data on both cryogenic and conventional fluids with extremely large volumes will be taken and compared.

(2) Secondly, a least upper bound for λ^* will be derived as well as an exact numerical solution for λ^* .

VAPOR INSTABILITIES

The total vaporization time for a drop is that time required for the entire volume of liquid which is placed on a heating surface to vaporize completely. The vaporization times of large water, ethanol, and nitrogen drops were measured on a 20.32 cm diameter - 1.9 cm thick brass plate which was instrumented with chromel-alumel thermocouples. The maximum size of drop investigated was 100 ml, which appreciably extends the range of the largest volumes investigated previously (i. e., 30 ml by Borishansky (ref. 7)). The plate was heated by a rheostat controlled hot plate.

A plot of the experimental data is shown in figure 1. In this figure, the dimensionless vaporization time t^* is plotted against the dimensionless initial volume V^* . The triangular data points are for nitrogen taken in reference 1 plus a few additional points (marked with a diamond) taken in the present study. As can be seen in figure 1, the dimensionless volume

runs from 100 to over 34 000, appreciably extending the range of dimensionless volumes investigated in reference 1. The actual volume of the nitrogen runs from 0.16 cm^3 to 40 cm^3 . The extremely large dimensionless volumes for nitrogen occurs because of its small value of surface tension in the property group that makes up the dimensionless volume V^* . From the experiments and theory discussed in reference 8, vapor breakthrough can occur for V^* greater than 100, that is, the entire range of dimensionless volumes shown in figure 1. However, breakthrough will be more pronounced for dimensionless volumes greater than 1000. The dimensionless volume V^* is a logical parameter to correlate vapor breakthrough since the property group used to dimensionalize the actual volume is proportional to the cube of the critical wavelength from hydrodynamic stability theory. In reference 8, breakthrough has been shown to be related to the critical wavelength.

In the present experimental study, the vaporization times of water and ethanol were measured with dimensionless volumes comparable to that of nitrogen. However, because of the relatively high value of surface tension of water and ethanol (as compared to nitrogen), actual liquid volumes from 25 to 100 cc were used. The basic purpose of the present experiment was to see if the data on the ordinary fluids would group together with the nitrogen data on a $V^* - t^*$ plot. Since the departure of the nitrogen data from the theoretical predictions of reference 5 was hypothesized in reference 1 to occur because of vapor breakthrough effects, a grouping of data would tend to lend further credibility to such a hypothesis.

As can be seen in figure 1, however, the ordinary fluids do not group with the nitrogen data. The increased amount of vapor breakthrough occurring in extended masses of ordinary fluids does not appear to appreciably increase the rate of heat transfer to those drops. Consequently, vapor breakthrough may not be the reason for the shorter vaporization times of the nitrogen drops.

LIMITING CASE FOR INFINITE DROPS

In this section, we will make a theoretical estimate of the effect of vapor breakthrough on film boiling of extremely large drops. First, we

notice a peculiarity of the expression for the heat transfer coefficient of the extended drop model. From table I,

$$h^* = \frac{1.64}{V^{*1/4}} \quad V^* > 155 \quad (3)$$

The derivation of this equation given in references 5 and 9 assumes a flat disk liquid drop with a uniform vapor gap beneath it, as pictured in the figure in the upper left corner of figure 1. However, for large volumes the drop will look more like the lower right hand schematic in figure 1, similar to conventional pool film boiling, except that the fluid depth is not appreciable.

As can be seen from equation (3), as V^* approaches infinity, the expression for the heat transfer coefficient will approach zero. Intuitively, however, we should expect the heat transfer coefficient to be related to conventional pool film boiling from a flat surface. The expression for pool film boiling heat transfer coefficient h_{fp} is given in reference 10 as follows:

$$h_{fp} = 0.410 \left[\frac{k^3 \lambda^* (\rho_L - \rho_V) \rho_V g}{\Delta T \mu L} \right]^{1/4} \quad (4)$$

Nondimensionalizing equation (4) using the property group in table I gives (neglect difference between λ^* in equation (4) and that used in equation (2))

$$h_{fp}^* = 0.410 \quad (5)$$

Taking the ratio of equations (3) and (5) gives

$$\frac{h_{fp}^*}{h^*} = 0.25 V^{*1/4} \quad (6)$$

Consequently, the break-even point ($h_{fp}^* = h^*$) occurs at V^* equal to 256. For dimensionless volumes greater than 256, equation (4) will give a higher value for the heat transfer coefficient. It must be pointed out, that equation (4) will be only an approximation to the actual value of the heat transfer coefficient, since pool film boiling (to which eq. (4) applies) implies a substantial liquid depth, whereas large unconstrained liquid masses have an asymptotic thickness (depth) on the order of 0.2 inch at most.

Nevertheless, let us use equation (5) in place of equation (3) in the derivation for the dimensionless vaporization time t^* when V^* is greater than 256. Following the detailed procedure given in reference 5, the vaporization time equation can be expressed as follows:

$$t^* = 4.5 \ln \left(\frac{V^*}{14.2} \right) \text{ for } V^* > 256 \quad (7)$$

This equation is represented by the dotted line in figure 1.

Intuitively, as the size of the liquid drop increases, the boiling model in the upper left hand corner of figure 1 will be transformed to the lower right hand model in figure 1. Consequently, one might expect the data points to shift from the upper to the lower curve. Perhaps the point where the shift occurs is different for different fluids. If this were true, the explanation given by Keshock and Bell (ref. 1), relative to nitrogen data at least, may be valid.

From high speed movie studies, the vapor domes in nitrogen appear to break open and spew out the enclosed vapor. However, in the water drops the domes sometimes remain intact much like a balloon. Perhaps, the higher surface tension of water relative to nitrogen accounts for the spread between the nitrogen and water data in figure 1. Thus, surface tension effects could cause a shift in the boiling model, as will be discussed in the discussion section of this report.

EFFECT OF LARGE CONVECTION HEATING

In determining the heat transfer coefficients given in table I, the energy equation and boundary conditions in reference 8 were taken as

$$\omega \frac{\partial T}{\partial z} = \alpha \frac{\partial^2 T}{\partial z^2} \quad (8)$$

$$z = 0 \quad T = T_p \quad (9)$$

$$z = \delta \quad T = T_{\text{sat}} \quad (10)$$

where a flat uniform vapor gap thickness δ has been assumed (see fig. 2). The radial convection term in equation (8) has been assumed small and

thus neglected. The temperature T_p is the supporting plate temperature and T_{sat} is the saturation temperature of the liquid drop. The convective velocity ω is directed downward from the surface of the liquid drop. It was found by a solution of the momentum equations to be of the form

$$\omega = -\frac{4\pi}{3} \frac{V}{A^2} (\rho_L - \rho_v) \frac{g}{\mu} \left(\frac{3}{2} \delta z^2 - z^3 \right) \quad (11)$$

where A is the cross sectional area of a drop of volume V .

Equations (8) to (11) are incomplete in that the vapor gap thickness δ is not specified. However, an energy balance at the interface yield an additional equation.

$$-\rho_v \lambda \omega(\delta) = -k \left. \frac{\partial T}{\partial z} \right|_{z=\delta} \quad (12)$$

In equation (12), the right hand side represents the heat conducted to the interface while the left hand side represents the equivalent latent heat removed from the interface.

Equations (8) to (11) can be solved to yield the following expression for the temperature distribution and gradient

$$\frac{T - T_p}{T_{sat} - T_p} = \frac{\int_0^{z/\delta} \exp \left[-\beta \left(\eta^3 - \frac{\eta^4}{2} \right) \right] d\eta}{\int_0^1 \exp \left[-\beta \left(\eta^3 - \frac{\eta^4}{2} \right) \right] d\eta} \quad (13)$$

$$\left. \frac{\partial T}{\partial z} \right|_{z=\delta} = \frac{(T_{sat} - T_p)}{\delta} \frac{\exp \frac{-\beta}{2}}{\int_0^1 \exp \left[-\beta \left(\eta^3 - \frac{\eta^4}{2} \right) \right] d\eta} \quad (14)$$

where a dimensionless gap thickness is defined as

$$\beta = \left[\frac{2\pi V(\rho_L - \rho_V)g}{3A^2 \alpha \mu} \right] \delta^4 = \frac{2\pi}{3} \left(\frac{V^*}{A^{*2}} \right) \left(\frac{C_p \Delta T}{\lambda^+} \right) \delta^{*4} \quad (15)$$

with δ^* defined in table I. Substituting equation (14) into equation (12) yields

$$\left(\frac{\lambda}{C_p \Delta T} \right) \beta = \frac{e^{-\beta/2}}{\int_0^1 \frac{1}{e^{-\beta \left(\eta^3 - \frac{\eta^4}{2} \right)} d\eta}} \quad (16)$$

Thus, the dimensionless gap thickness β is only a function of the parameter $(\lambda/C_p \Delta T)$.

The heat transfer coefficient to the drop h is defined at the liquid vapor interface as follows:

$$h(T_p - T_{sat}) = q = -\rho_V \lambda \omega(\delta) \quad (17)$$

Substituting in the expression for $\omega(\delta)$ from equation (11) into equation (17), introducing the parameter β from equation (15) and expressing the V and A in terms of V^* and A^* in table I give the expressions for the heat transfer coefficients shown in table I with λ^* in the dimensionless property group defined as

$$\lambda^* = \lambda \left(\frac{\lambda}{C_p \Delta T} \beta \right)^3 \quad (18)$$

where β can be found from a solution of equation (16) for various values of $C_p \Delta T/\lambda$ as the parameter.

Exact Solution for λ^*

Equation (16) was solved numerically to determine the value of β for various values of $(C_p \Delta T/\lambda)$. A half-interval search technique in conjunction with a Simpson rule integration was used. The value of β was then substituted into equation (18) to determine λ^* . Since the dimensionless vaporization time t^* as well as the heat transfer coefficient are proportional to $(\lambda^*)^{1/4}$, the fourth root of λ^*/λ is plotted in figure 3 instead of λ^*/λ .

Small $C_p \Delta T / \lambda$

For small values of $C_p \Delta T / \lambda$, the exponential in equation (16) can be approximated by

$$e^{-x} \approx 1 - x \quad (19)$$

Using this approximation in equation (16), solving for β , and substituting the value for β into equation (18) yields

$$\lambda_{\text{small}}^* = \lambda \left[1 + \frac{7}{20} \frac{C_p (T_p - T_{\text{sat}})}{\lambda} \right]^{-3} \quad (20)$$

This was the value used in the correlation of the data in figure 1. The fourth root of $\lambda_{\text{small}}^* / \lambda$ is also plotted in figure 3.

Maximum λ^*

The integral in the denominator of equation (16) cannot be evaluated in closed form. Consequently, the numerical and exponential approximations were necessary. However, another interesting solution for λ^* can be obtained by noting that

$$e^{-\beta(\eta^3 - \eta^4/2)} \geq e^{-\beta\eta/2} \quad 0 \leq \eta \leq 1 \quad (21)$$

The expressions are equal at η equals 0 and 1. Therefore,

$$\left(\frac{\lambda}{C_p \Delta T} \right) \beta < \frac{e^{-\beta/2}}{\int_0^1 e^{-\beta\eta/2} d\eta} \quad (21)$$

Solving equation (21) for β and substituting the expression for β into equation (18) yield

$$\lambda^* < \lambda \left[\frac{\ln \left(1 + \frac{C_p \Delta T}{2\lambda} \right)}{\frac{C_p \Delta T}{2\lambda}} \right]^3 \equiv \lambda_{\text{max}}^* \quad (22)$$

The fourth root of λ_{\max}^*/λ is also plotted in figure 3. As seen in this figure, λ_{\max}/λ is always greater than the exact solution.

Surprisingly, however, the ratio of the fourth root of the exact to maximum solution is nearly a constant over a very large range of $C_p \Delta T/\lambda$. This is seen in figure 3 by noting that the curves for $\lambda(\text{exact})$ and λ_{\max} are parallel. Consequently, the following slight modification of λ_{\max} (eq. (22)) is made to give a good curve fit to the exact solution when $C_p \Delta T/\lambda$ is large:

$$\lambda_{\text{cr}}^* = \lambda \left[\frac{0.874 \ln \left(1 + \frac{C_p \Delta T}{2\lambda} \right)}{\frac{C_p \Delta T}{2\lambda}} \right]^3 \quad \text{for } \frac{C_p \Delta T}{\lambda} > 2 \quad (23)$$

As can be seen in figure 3, for large values of the parameter $C_p \Delta T/\lambda$, the effect of convection heating becomes very important. The approximation λ_{small} should not be used in this case, rather, the numerical results or the curve fit given by equation (23) should be used. The $C_p \Delta T/\lambda$ will increase at higher system pressures, especially near the thermodynamic critical point.

The nitrogen data in figure 1 has a $C_p \Delta T/\lambda$ value near 1. In this range the approximation for λ^* by λ_{small}^* is still quite good. Consequently, the nitrogen data in figure 1 when corrected for the exact value of λ^* moved upward by only about 3 percent. This is an improvement in the theory; however, the correction is still small compared to the 30 percent deviation between the theoretical and experimental data.

DISCUSSION

Vapor breakthrough has been shown to be relatively small for the present set of data for ordinary fluids as shown in figure 1, although vapor breakthrough may still account for some of the downward shift in the experimental points for liquid nitrogen. A new theoretical curve which accounts for vapor breakthrough (shown dotted in fig. 1) has been developed that seems to correlate the nitrogen data.

Convection heating effects, represented by the λ^* correction term, are relatively small for the temperatures and pressure (atmospheric) investigated in this experiment. However, convection effects are likely to be more significant for higher temperatures and pressures near the critical point.

At present, the precise reasons for the downward shift in the nitrogen data in figure 1 has not been established. The most likely reason, at present, appears to be surface tension effects on the vapor dome. Water with a high value of surface tension tends to prevent the vapor from breaking through the domes, while nitrogen with a small value of surface tension allows the vapor domes to spew out the vapor. Thus, the flat disk model (upper curve in fig. 1) best approximates water and high surface tension fluid, while the breakthrough model (lower dotted curve in fig. 1) best approximates nitrogen and lower surface tension fluids.

In order to fully explain the anomalous results observed in figure 1, investigation of other possible causes for such behavior is warranted. Three such areas worthy of further investigation are surface tension effects, mass transfer from the top of the drop and slip at the liquid vapor interface. The no slip boundary condition assumes the radial component of vapor velocity u (see fig. 2) is zero at the liquid vapor interface. This assumption works well for ordinary fluids. However, perhaps the relatively large difference in surface tension between ordinary fluids and the cryogen could alter the boundary condition. Wachters (ref. 3) shows that for the complete slip boundary condition the heat transfer coefficient increases by 40 percent. Consequently, a change in the boundary condition from slip to partial slip would improve the correlation, although justification for this partial slip boundary condition has not been physically established.

As part of the present study, data was taken for large masses of water with surface tension additives. The data were correlated onto the plot using the value of the surface tension data without additives. If the correct value of σ were known, the data point would shift to the right and upward. The strong downward trend in the water data point at a dimensionless volume

6000, however, indicates that perhaps surface tension effects should be investigated in more detail.

Presently, the reason for the separation between the data for ordinary fluids and the cryogen remains unknown, in the sense that a variety of causes could produce the effect.

CONCLUSIONS

The principle conclusions of the present study are

1. For large values of the parameter $C_p \Delta T / \lambda$ the following expression should be used for the modified latent heat of vaporization

$$\lambda_{cr}^* = \lambda \left[\frac{0.874 \ln \left(1 + \frac{C_p \Delta T}{2\lambda} \right)}{\frac{C_p \Delta T}{2\lambda}} \right]^3 \quad \text{for } \frac{C_p \Delta T}{\lambda} > 2$$

This expression would also be used for conventional pool film boiling problems.

2. For very large liquid nitrogen drops in film boiling, the following new expression has been found to correlate the vaporization time:

$$t^* = 4.5 \ln \left(\frac{V^*}{14.2} \right) \quad \text{for } V^* > 256$$

3. Large differences in surface tension could have pronounced effects on the film boiling mechanism.




REFERENCES

1. Keshock, E. G.; and Bell, K. J.: Heat Transfer Coefficient Measurements of Liquid Nitrogen Drops Undergoing Film Boiling. Presented at 1969 Cryogenic Engineering Conference, Los Angeles, Calif.
2. Bell, K. J.: The Leidenfrost Phenomenon: A Survey. Chem. Eng. Progr. Symp. Ser., vol. 63, no. 79, 1967, pp. 73-82.
3. Wachters, L. H. J.: Heat Transfer From a Hot Wall to Drops in a Spheroidal State. Doctoral Thesis, Tech. Univ. Delft, Netherlands, 1965.

4. Forslund, R. P.; and Rohsenow, W. M.: Dispersed Flow Film Boiling. *J. Heat Transfer*, vol. 90, no. 4, Nov. 1968, pp. 399-407.
5. Baumeister, Kenneth J.; Hamill, Thomas D.; and Schoessow, Glen J.: A Generalized Correlation of Vaporization Times of Drops in Film Boiling on a Flat Plate. *Proceedings of the Third International Heat Transfer Conference*. Vol. 4. AIChE, 1966, pp. 66-73.
6. Baumeister, K. J.: Comments to reference 1 presented at the 1969 Cryogenic Engineering Conference, Los Angeles, Calif.
7. Borishansky, V. M.: Problems of Heat Transfer During a Change of State: A Collection of Articles. S. S. Kutateladze, ed. Rep. AEC-tr-3405, 1953, pp. 109-144.
8. Patel, B. M.; and Bell, K. J.: The Leidenfrost Phenomenon for Extended Liquid Masses. *Chem. Eng. Progr. Symp. Ser.*, vol. 62, no. 64, 1966, pp. 62-71.
9. Baumeister, Kenneth J.; and Hamill, Thomas D.: Creeping Flow Solution of the Leidenfrost Phenomenon. NASA TN D-3133, 1965.
10. Hamill, Thomas D.; and Baumeister, Kenneth J.: Film Boiling Heat Transfer from a Horizontal Surface as an Optimal Boundary Value Process. *Proceedings of the Third International Heat Transfer Conference*. Vol. 4 AIChE, 1966, pp. 59-65.

TABLE I. - SUMMARY TABLE FOR LEIDENFROST DROP RESULTS FROM REFERENCE 5

[Effect of vapor density on drop shape and drop buoyancy has been included in this table. It was not included in reference 5.]

Dimensionless volume range, $V^* = \frac{V}{L^3}$	Drop shape	Dimensionless average drop thickness, $l^* = \frac{l}{L}$	Dimensionless area, $A^* = \frac{A}{L^2}$	Dimensionless vapor gap thickness beneath drop, $\delta^* = \frac{\delta}{\left(\frac{k \Delta T \mu L}{\lambda^* (\rho_L - \rho_v) \rho_v g} \right)^{1/4}}$	Dimensionless heat transfer coefficient, $h^* = \frac{h}{\left(\frac{k^3 \lambda^* (\rho_L - \rho_v) \rho_v g}{\Delta T \mu L} \right)^{1/4}}$	Dimensionless vaporization time $t^* = \frac{t}{\lambda \rho_L \left(\frac{\mu L^5}{k^3 \lambda^* g (\rho_L - \rho_v) \rho_v \Delta T^3} \right)^{1/4}}$
$V^* < 0.8$	Small spheroid 	$l^* = 0.83V^{*1/3}$	$A^* = 1.81V^{*2/3}$	$\delta^* = 0.91V^{*1/12}$	$h^* = 1.1V^{*-1/12}$	$t^* = 1.21V^{*5/12}$
$0.8 < V^* < 155$	Large drop 	$l^* = 0.8V^{*1/6}$	$A^* = 1.25V^{*5/6}$	$\delta^* = 0.93V^{*-1/6}$	$h^* = 1.075V^{*1/6}$	$t^* = 2.23V^{*1/3} - 0.97$
$V^* > 155$	Extended drop (constant thickness) 	$l^* = 1.85$	$A^* = 0.54V^*$	$\delta^* = 0.61V^{*1/4}$	$h^* = 1.64V^{*-1/4}$	$t^* = 4.52V^{*1/4} - 5$

where

$$L = \left(\frac{\sigma \gamma_c}{(\rho_L - \rho_v)g} \right)^{1/2}$$

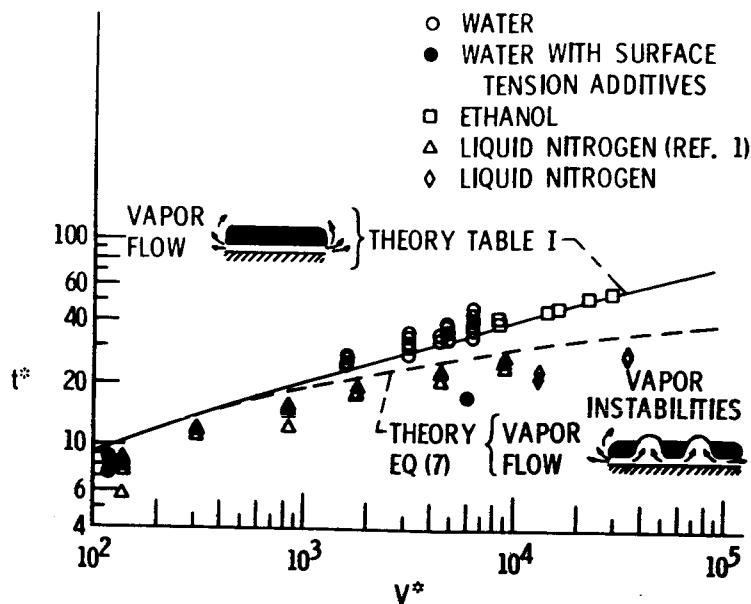


Figure 1. - Total vaporization time correlation.

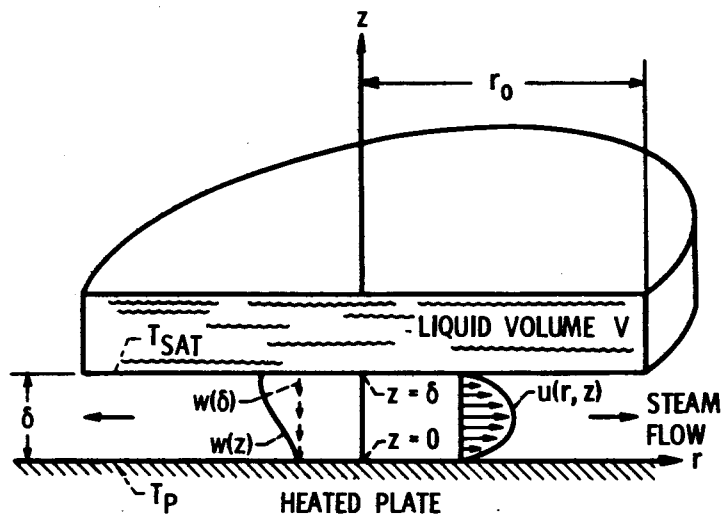


Figure 2. - Schematic model of the evaporation of a flat disk.

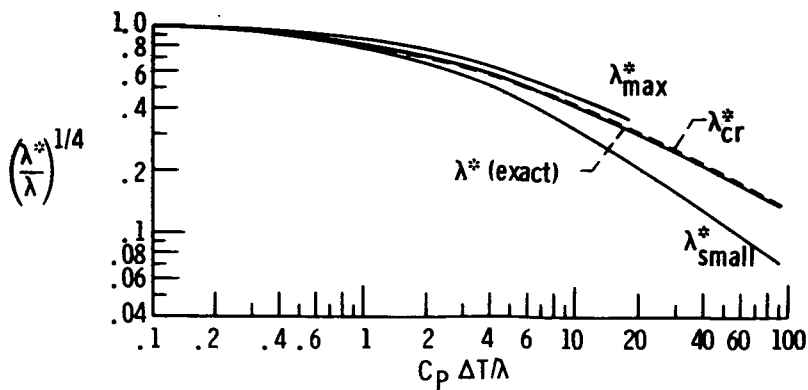


Figure 3. - Comparison of modified latent heats of vaporization.